Al-Qadisiyah Journal of Pure Science

Volume 26 | Number 4 Article 36

8-15-2021

Radiation And Mass Transfer Effects On Inclined MHD Oscillatory Flow for Prandtl-Eyring Fluid through a Porous Channel

Dheia G. Salih Al-Khafajy
Department of Mathematics, College of Science, University of Al-Qadisiyah, Diwaniyah, Iraq,
dheia.salih@qu.edu.iq

Wedyan Abed Muhi Al-Kaabi
Department of Mathematics, College of Science, University of Al-Qadisiyah, Diwaniyah, Iraq,
waddyanabed@gmail.com

Recommended Citation

Al-Khafajy, Dheia G. Salih and Al-Kaabi, Wedyan Abed Muhi (2021) "Radiation And Mass Transfer Effects On Inclined MHD Oscillatory Flow for Prandtl-Eyring Fluid through a Porous Channel," *Al-Qadisiyah Journal of Pure Science*: Vol. 26: No. 4, Article 36.
DOI: 10.29350/qjps.2021.26.4.1397
Available at: https://qjps.researchcommons.org/home/vol26/iss4/36

Al-Qadisiyah Journal of Pure Science
ISSN(Printed): 1997-2490 ISSN(Online): 2411-3514
DOI: /10.29350/jops.
http://qu.edu.iq/journalsc/index.php/JOPS

Radiation and Mass Transfer Effects on Inclined MHD Oscillatory Flow for Prandtl-Eyring Fluid through a Porous Channel

Authors Names
a. Dheia G. Salih Al-Khafajy
b. Wedyan A .Muhi Al-Kaabi

Article History
Received on:25/6/2021
Revised on:20/7/2021
Accepted on: 25/7/2021
Keywords:
Prandtl-Eyring fluid, the Soret numbe, the concentration, Grashof number

DOI: https://doi.org/10.29350/jops.2021.26. 4.1397

ABSTRACT

The aim of this research is to study the effect of heat transfer on the oscillating flow of the hydrodynamics magnetizing Prandtl-Eyring fluid through a porous medium under the influence of temperature and concentration for two types of engineering conditions "Poiseuille flow and Couette flow". We used the perturbation method to obtain a clear formula for fluid motion. The results obtained are illustrated by graphs.

1.Introduction:

Because of its wide variety of applications in nuclear engineering and industry, heat and mass transfer in boundary layer flow has gotten a lot of attention in recent years. These research' findings are utilized in modeling and simulation. Thermal and concentration boundary layers develop when a fluid of a particular temperature and concentration flows across a surface of a different temperature and concentration.

The behavior of non-Newtonian fluids in permeable media differs depending on the model used. The flow between parallel plates under the effect of the transverse magnetic field and heat transfer was examined by Nigamf and Singhj [11]. Raptis et al. [13] investigated hydro-magnetic free convection flow between two parallel plates in a porous medium. For the unstable flow of a thin fluid in, Hamza et al [4] addressed the impacts of the sliding state, as well as the transverse magnetic field and radiative heat transfer. Hussain et al. [5] suggested using a stretching cylinder with Newtonian heating to

[a] Department of Mathematics, College of Science, University of Al-Qadisiyah, Diwaniyah, Iraq, E-Mail: dr.dheia.g.salih@gmail.com , dheia.salih@qu.edu.iq
[b] Department of Mathematics, College of Science, University of Al-Qadisiyah, Diwaniyah, Iraq, E-Mail: waddyanabed@gmail.com

analyze the MHD flow of Prandtl-Eyring fluid. Lqaa and Dheia [9] investigated the effect of Heat Transfer MHD Oscillatory Flow for an Eyring-Powell Fluid with Variable Viscosity through a Porous Medium. Lqaa and Dheia [2] published Influence of Heat Transfer on MHD Oscillatory Flow for Eyring-Powell Fluid via a Porous Medium with Varying Temperature and Concentration. The goal of this study is to look at how heat transfer affects the oscillating flow of a magnetizing Prandtl-Eyring fluid through a porous material under the impact of temperature and concentration under two different engineering conditions: Poiseuille flow and Couette flow. See [3], [7], [12], [14], [15], [16]. Some studies have been conducted in the study of Prandtl-Eyring fluid, which is a non-Newtonian fluid, where the flow of this fluid has been studied in different conditions, different channels and at different times for several researchers, including [1], [6], [8], [10], [17].

Stimulated by this, assume a mathematical model for analyzing the effect of electrical conductivity on the oscillatory flow for Prandtl-Eyring fluid through the porous channel, in addition to studying the effect of fluid flow on its temperature.

2.Mathematical Formulation:

As shown in Figure 1, a Prandtl-Eyring fluid passes through an h-width channel under the effect of an electrically generated magnetic field and nuclear heat transfer. The fluid is thought to produce very little electromagnetic force and to have low electrical conductivity. In a Cartesian coordinate system, $(u(y,t),0,0)$ is a velocity vector in which u represents the x-component of velocity and y is perpendicular to the x-axis. .

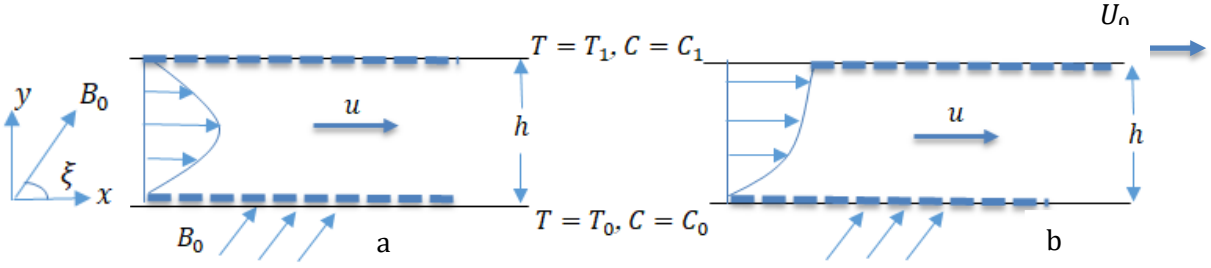

Figure 1 Channel format : (a) Poiseuille flow and (b) Couette flow.

3.Basic Equations:

The basic equations that control the Pradtl-Eyring fluid are as follows:

The equation for continuity is:

$$\frac{\partial \bar{u}}{\partial \bar{x}} + \frac{\partial \bar{v}}{\partial \bar{y}} = 0. \qquad (1)$$

The momentum equations are:

In the x – direction:

$$\rho\left(\frac{\partial \bar{u}}{\partial \bar{t}}+\bar{u}\frac{\partial \bar{u}}{\partial \bar{x}}+\bar{v}\frac{\partial \bar{u}}{\partial \bar{y}}\right)=-\frac{\partial \bar{p}}{\partial \bar{x}}+\frac{\partial \bar{\tau}_{\bar{x}\bar{x}}}{\partial \bar{x}}+\frac{\partial \bar{\tau}_{\bar{x}\bar{y}}}{\partial \bar{y}}+\rho g\beta_T\,(T-T_0)+\rho g\beta_C(C-C_0)-\sigma B_0^2 Sin^2(\xi)\bar{u}-\frac{\mu_0}{k}\bar{u}. \quad (2)$$

In the y – direction:

$$\rho\left(\frac{\partial \bar{v}}{\partial \bar{t}}+\bar{u}\frac{\partial \bar{v}}{\partial \bar{x}}+\bar{v}\frac{\partial \bar{v}}{\partial \bar{y}}\right)=-\frac{\partial \bar{p}}{\partial \bar{y}}+\frac{\partial \bar{\tau}_{\bar{y}\bar{x}}}{\partial \bar{x}}+\frac{\partial \bar{\tau}_{\bar{y}\bar{y}}}{\partial \bar{y}}-\frac{\mu_0}{k}\bar{v}. \quad (3)$$

The temperature equation is given by:

$$c_T\rho\left(\frac{\partial T}{\partial \bar{t}}+\bar{u}\frac{\partial T}{\partial \bar{x}}+\bar{v}\frac{\partial T}{\partial \bar{y}}\right)=K_T\left(\frac{\partial^2 T}{\partial \bar{x}^2}+\frac{\partial^2 T}{\partial \bar{y}^2}\right)-\frac{\partial q}{\partial y}+Q_H(T-T_0). \quad (4)$$

The concentration equation is given by:

$$\frac{\partial C}{\partial \bar{t}}=D\frac{\partial^2 C}{\partial \bar{y}^2}-K_r^*(C-C_0)+\frac{DK_{Tt}}{T_m}\frac{\partial^2 T}{\partial \bar{y}^2}. \quad (5)$$

where $V\equiv(u(y,t),0,0)$ is the velocity field, $T(y,t)$ is a fluid temperature, B_0 is a magnetic field strength, ρ is a fluid density, σ is a conductivity of the fluid**,** k is a permeability, c_{T} is a specific heat at constant pressure, K_T is a thermal conductivity, q is a radioactive heat flux, Q_H is heat generation, C is the concentration, D is the coefficient of mass diffusivity, $(0\le\xi\le\pi)$ is the angle between velocity field and magnetic field strength and K_{Tt} is the thermal diffusion ratio. The corresponding boundary conditions are given below:

$$T=T_0\,,\mathrm{C}=C_0 \text{ at } \bar{y}=0 \text{ and } T=T_1,\mathrm{C}=C_1 \text{ at } \bar{y}=h \quad (6)$$

The radioactive heat flux is given by:

$$\frac{\partial q}{\partial y}=4\eta^2(T_0-T) \quad (7)$$

The radiation absorption denoted by η.

The fundamental equation for Prandtl - Eyring fluid is given as:

$$\boldsymbol{S}=-\bar{p}\boldsymbol{I}+\tau \quad (8)$$

$$\tau=\frac{B}{\dot{\gamma}}sinh^{-1}\left(\frac{\dot{\gamma}}{C}\right)\Upsilon\,,\dot{\gamma}=\sqrt{\frac{\mathbf{1}}{\mathbf{2}}tr\,(\Upsilon)^2}\,,\ \Upsilon=\nabla\bar{V}+(\nabla\bar{V})^T \quad (9)$$

$\nabla\bar{V}=\begin{bmatrix}u_x & u_y & u_z\\ v_x & v_y & v_z\\ w_x & w_y & w_z\end{bmatrix}$, $(\nabla\bar{V})^T=\begin{bmatrix}u_x & v_x & w_x\\ u_y & v_y & w_y\\ u_z & v_z & w_z\end{bmatrix}$ The Rivlin-Ericksen tensors are given as $\Upsilon=\nabla\bar{V}+(\nabla\bar{V})^T$, where $(\nabla\bar{\mathrm{V}})$ is the velocity field in the cartesian coordinates system (x,y,z) and $(\nabla\bar{\mathrm{V}})^{\mathrm{T}}$ is the transpose of the velocity field.

The stress component is given by:

$$\bar{\tau}_{\bar{x}\bar{x}} = \bar{\tau}_{\bar{y}\bar{y}} = 0 \text{ and } \bar{\tau}_{\bar{x}\bar{y}} = \bar{\tau}_{\bar{y}\bar{x}} = \sqrt{2}\, B\left(\frac{1}{A}\frac{\partial \bar{u}}{\partial \bar{y}} - \frac{1}{6}\left(\frac{1}{A}\frac{\partial \bar{u}}{\partial \bar{y}}\right)^3\right) \quad (10)$$

$$\text{And} \quad \bar{\tau}.(grad\, \bar{V}) = \bar{\tau}_{\bar{x}\bar{y}}\frac{\partial \bar{u}}{\partial \bar{y}}. \quad (11)$$

4. **Method of Solution:**

We can introduce non-dimensional circumstances to the governing equations of motion as follows:

$$\left.\begin{array}{c} x = \frac{\bar{x}}{h}, y = \frac{\bar{y}}{h}, u = \frac{\bar{u}}{U}, t = \frac{\bar{t}U}{h}, p = \frac{\bar{p}h}{\mu_0 U}, \\ \Delta C = C_1 - C_0, \Delta T = T_1 - T_0, \theta = \frac{T-T_0}{\Delta T}, \Phi = \frac{\mathrm{C}-\mathrm{C}_0}{\Delta C}, \tau_{xy} = \frac{h}{\mu_0 U}\bar{\tau}_{\overline{xy}}. \end{array}\right\} \quad (12)$$

where U is the mean flow velocity.

With $\theta = 0, \Phi = 0$, at $y = 0$ and $\theta = 1, \Phi = 1$, at $y = 1$.

implies that

$$\rho\frac{Uh}{\mu_0}\frac{\partial u}{\partial t} = -\frac{dp}{dx} + \frac{\partial \tau_{xy}}{\partial y} + \frac{\rho g \beta_T h^2 \Delta T\theta}{\mu_0 U} + \frac{\rho g \beta_C h^2(\Delta C)\Phi}{\mu_0 U} - \frac{\sigma B_0^2 Sin^2(\xi)u}{\mu_0 h^2} - \frac{h^2}{k}u, \quad (13)$$

$$\frac{\rho C_T h U}{K}\Delta T \;\; \frac{\partial \theta}{\partial t} = \Delta T\frac{\partial^2 \theta}{\partial y^2} + \frac{4\eta^2 h^2}{k}\Delta T\theta + Q\Delta T\theta. \quad (14)$$

$$\frac{\partial \Phi}{\partial t} = \frac{1}{S_c}\frac{\partial^2 \Phi}{\partial y^2} - K_r\Phi + \frac{DK_T\,\Delta T}{T_m h U(C_1 - C_0)}\frac{\partial^2 \theta}{\partial y^2}. \quad (15)$$

Substituting equation (12) into equations (1) - (7) and (10), we have the following of non- dimensional equations will by gained as follows;

$$Re\frac{\partial u}{\partial t} = -\frac{\partial p}{\partial x} + \sqrt{2}\mathcal{F}\frac{\partial^2 u}{\partial y^2} - 3\sqrt{2}\mathcal{S}\left(\frac{\partial u}{\partial y}\right)^2\frac{\partial^2 u}{\partial y^2} + Gr\theta + Gc\Phi - \left(M_2^2 + \frac{1}{Da}\right)u \quad (16)$$

$$Pe \;\; \frac{\partial \theta}{\partial t} = \frac{\partial^2 \theta}{\partial y^2} + (N^2 + Q)\theta. \quad (17)$$

$$\frac{\partial \Phi}{\partial t} = \frac{1}{S_c}\frac{\partial^2 \Phi}{\partial y^2} - K_r\Phi + Sr\frac{\partial^2 \theta}{\partial y^2}, \quad (18)$$

where $M_2 = MSin(\xi)$

$Re = \frac{\rho h U}{\mu_0}$ is a Reynolds number, $Da = \frac{k}{h^2}$ is a Darcy number, $M = \sqrt{\frac{\sigma B_0^2 h^2}{\mu_0}}$ is a magnetic parameter, $Pe = \frac{\rho h U c_T}{K_T}$ is a Peclet number, $N = \sqrt{\frac{4\eta^2 h^2}{K_T}}$ is the radiation parameter, $Gr = \frac{\rho g \beta h^2 \Delta T}{\mu_0 U}$ is a Grashof

number, $Pr = \frac{\mu_0 c_T}{K_T}$ is a Prandtl number, $Ec = \frac{U^2}{c_T \Delta T}$ is an Eckert number, $K_r = \frac{hKr^*}{U}$ Chemical reaction parameter, $Br = PrEc$ Brinkman number, $Sr = \frac{DK_T(T_1 - T_0)}{UT_m h(C_1 - C_0)}$ is the Soret numbe,$Gc = \frac{\rho g \beta_C h^2 (C_1 - C_0)}{\mu_0 U}$, is solutal Grashof number, $Q = \frac{Q_H h^2}{K}$ is the heat generation parameter, $M_2^2 = \frac{\sigma B_0^2 h^2}{\mu_0} \mathrm{Sin}^2(\xi)$, $Sc = \frac{Uh}{D}$ is the Schmidt number, and $\left(\mathcal{F} = \frac{B}{\mu_0 A}, \mathcal{S} = \frac{\mathcal{F} U^2}{6h^2 A^2}\right)$ are the dimensionless Prandtl-Eyring fluid parameters.

The temperature equation and the concentration equation both include boundary conditions $\left\{ \begin{array}{l} \theta\Delta T + T_0 = T_0, \Phi\Delta C + C_0 = C_0, \text{at } yh = 0 \\ \theta\Delta T + T_0 = T_1, \Phi\Delta C + C_0 = C_1, \text{at } yh = 0. \end{array} \right\}$

5.Solution of the problem:

5.1.Solution of the temperature equation

To solve the heat equation (17) with associative boundary conditions $\theta(0) = 0, \theta(1) = 1$. Let $\theta(y,t) = \theta_0(y)e^{i\omega t}$ and by substituting into equation (17), after simplifying the result, we obtain

$$\frac{d^2\theta_0}{dy^2} + (N^2 + Q - i\omega Pe)\theta_0 = 0 \quad (19)$$

Therefore, the temperature function is :

$$\theta(y,t) = \csc(Z)\sin(Zy)e^{i\omega t} \quad (20)$$

where $Z = \sqrt{N^2 + Q - i\omega Pe}$

5.2. Solution of the concentration equation;

To solve the concentration equation (18) with boundary conditions:
$\Phi(0) = 0$, $\Phi(1) = 1$. Let $\Phi(y,t) = \Phi_0(y)e^{i\omega t}$. Substituting equations (18) after simplifying the result, we obtain

$$\frac{d^2\Phi_0}{dy^2} - Sc(K_r + i\omega)\Phi_0 = -Sc\, Sr \frac{d^2\theta_0}{dy^2}. \quad (21)$$

Therefore, the concentration equation function is :

$$\Phi(y,t) = e^{i*\omega*t} * \left(e^{\sqrt{B}y}\left[\frac{e^{\sqrt{B}-it\omega}(B+P+P\mathrm{ScSr})}{(-1+e^{2\sqrt{B}})(B+P)}\right] + e^{-\sqrt{B}y}\left[-\frac{e^{\sqrt{B}-it\omega}(B+P+P\mathrm{ScSr})}{(-1+e^{2\sqrt{B}})(B+P)}\right] - \frac{e^{-it\omega}P\mathrm{ScSrCsc}[\sqrt{P}]\mathrm{Sin}[\sqrt{P}y]}{B+P}\right).$$

(22)

Where $B = Sc(K_r + i\omega)$, $P = N^2 + Q - i\omega\mathrm{Pe}$.

5.3.Solution of the momentum equation

There are two forms of flow in this section: Poiseuille flow and Couette flow.

A.Poiseuille flow

By above assumption (no-slip) condition the boundary conditions are $\bar{u} = 0$ at $\bar{y} = 0, h$. From equations (16) the non-dimensional boundary conditions are $u(0) = u(1) = 0$.

From equation (3), we have $\frac{\partial p}{\partial y} = 0$, so the pressure p depends on x only. Set ω be an oscillation of frequency, and let

$$-\frac{dp}{dx} = \lambda e^{i\omega t} \quad , \quad u(y,t) = u_0(y)e^{i\omega t} \tag{23}$$

where λ is a real constant.

By Substituting equations (23) by equation (16), we have

$$-\lambda = \sqrt{2}\mathcal{F}\frac{\partial^2 u_0(y)}{\partial y^2} - 3\sqrt{2}e^{2i\omega t}\mathcal{S}\left(\frac{\partial^2 u_0(y)}{\partial y^2}\right)\left(\frac{\partial u_0(y)}{\partial y}\right)^2 + Gr\theta_0 + Gc\Phi_0 - \left(i\omega Re + M_2^2 + \frac{1}{Da}\right)u_0(y) \tag{24}$$

With boundary condition $u_0(0) = u_0(0) = 0$,

The equation (24) is a nonlinear differential equation and it is hard to find an exact solution, so will use the perturbation technique to find the solution of the equation, as follows:

$$u_0 = u_{00} + \mathcal{S}\, u_{01} + O(\mathcal{S}^2) \ . \tag{25}$$

By substituting equation (25) into equation (24), with boundary conditions $u_0(0) = u_0(1) = 0$, then equating the like powers of $\mathcal{S}$, we obtain the following results presented in the forthcoming subsections:

***i* - Zeros-order system ($\mathcal{S}^0$)**

$$\frac{\partial^2 u_{00}}{\partial y^2} - \frac{\left(i\omega Re + M_2^2 + \frac{(1)}{Da}\right)u_{00}}{\sqrt{2}\mathcal{F}} = \frac{-(\lambda + Gr\theta_0 + Gc\Phi_0)}{\sqrt{2}\mathcal{F}}. \tag{26}$$

The boundary criteria are as follows: $u_{00}(0) = u_{00}(1) = 0$

***ii* – First - order system ($\mathcal{S}^1$)**

$$\frac{\partial^2 u_{01}}{\partial y^2} - \frac{\left(i\omega Re + M_2^2 + \frac{(1)}{Da}\right)u_{01}}{\sqrt{2}\mathcal{F}} = \frac{3}{\mathcal{F}}\, e^{2i\omega t}\left(\frac{\partial\, u_{00}}{\partial y}\right)^2\left(\frac{\partial^2 u_{00}}{\partial y^2}\right), \tag{27}$$

The associated boundary conditions are: $u_{01}(0) = u_{01}(1) = 0$

From the solution of equations (26) and (27), and the resulting substitution in equation (25) after substitution in equation (24), we obtain the solution of the equation of motion in the case of Poiseuille flow

As a result, the momentum equation solution for the

$$u(y,t) = e^{i*\omega*t} * \left(\frac{\mathrm{H}}{A} + e^{\sqrt{A}y}\left[-\frac{\mathrm{H}}{A(1+e^{\sqrt{A}})}\right] + e^{-\sqrt{A}y}\left[-\frac{\mathrm{H}e^{\sqrt{A}}}{A(1+e^{\sqrt{A}})}\right]\right) + \xi * \left(-\frac{3\mathrm{H}^3 e^{2it\omega}e^{-3\sqrt{A}y}(e^{3\sqrt{A}}+e^{6\sqrt{A}y}-4e^{2\sqrt{A}(1+y)}-e^{\sqrt{A}(1+4y)}+4\sqrt{A}e^{2\sqrt{A}(1+y)}y-4\sqrt{A}e^{\sqrt{A}(1+4y)}y)}{4\sqrt{2}A^2(1+e^{\sqrt{A}})^3\mathcal{F}} + e^{\sqrt{A}y}\left[\frac{3\mathrm{H}^3 e^{2it\omega}(1-e^{\sqrt{A}}-e^{2\sqrt{A}}-4\sqrt{A}e^{2\sqrt{A}}+e^{3\sqrt{A}})}{4\sqrt{2}A^2(1+e^{\sqrt{A}})^{4\mathcal{F}}}\right] + e^{-\sqrt{A}y}\left[\frac{3\mathrm{H}^3 e^{2it\omega}e^{\sqrt{A}}(1-4e^{\sqrt{A}}+4\sqrt{A}e^{\sqrt{A}}-4e^{2\sqrt{A}}+e^{3\sqrt{A}})}{4\sqrt{2}A^2(1+e^{\sqrt{A}})^{4\mathcal{F}}}\right]\right) \quad (28)$$

Where $A = \frac{\left(i\omega Re + M_2^2 + \frac{(1)}{Da}\right)}{\sqrt{2\mathcal{F}}}$, $\mathrm{H} = \frac{-(\lambda + Gr\theta_0 + Gc\Phi_0)}{\sqrt{2\mathcal{F}}}$

B.Couette flow

The only change between this portion of the equation (24) and the preceding part is the boundary condition, which becomes $u_0(0) = 0, u_0(1) = U_0 e^{-i\omega t}$. In Couette flow, we perform the same thing we did in Poiseuille flow. In the Couette flow, The solution has been calculated by the perturbation technique and the results have been discussed through graphs

6.Results and Discussion:

On the basis of some observations made during the graphics illustrations, the impact of fluid parameters on velocity and temperature in the MHD oscillatory flow of Prandtl-Eyring fluid through a porous medium for Poiseuille flow and Couette flow in order to have a clearer description of the physiological matter.

The (MATHEMATICA-12) program was used to collect the statistical solutions and graphs. The momentum equation is solved using the perturbation technique, and all of the results are graphed in area $0 \leq y \leq 1$, which is the diameter of the flow channel.

1. Figures (4-17)show the velocity profile. Each figure is divided into two halves, with (a) representing Poiseuille flow and (b) representing Couette flow, respectively. Each of these forms will be explained in terms of the two geometric types of flow states. The velocity profile u decreases as t increases, as seen in Figure 2. The velocity profile u rises as Gc increases, as seen in Figure 3. Figure 4 illustrates that as the parameters M are increased, the velocity profiles u decrease. Figure 5 illustrates that as the parameters Sc are increased, the velocity profiles u decrease. Figure 6 illustrates that as the parameters Sr are increased, the velocity profiles u decrease. The velocity profile u rises as N increases, as seen in Figure 7. Figure 8 demonstrates how the impact of Pe on velocity profiles u diminishes. The velocity profile u rises as Gr increases, as seen in Figure 9. The velocity profile u rises with the increasing $\mathcal{S}$ as seen in Figure 10 The velocity profile u rises as Da increases, as seen in Figure 11. Figure 12 demonstrates how the impact of F on velocity profiles u diminishes. Figure 13 illustrates that when the parameters are reduced, the velocity profiles u rise. Re. The impact on the velocity profiles function u vs. y is seen in Figure 14. It has been discovered that raising the velocity profiles of function u increase. 1. The velocity profiles u rise when the parameters are increased, as seen in Figure 15 Q. As seen in Figure 16, velocity profiles decrease as the parameters rise. The velocity profiles decrease as the parameters rise, as seen in Figure 17. Figures (2- 17) illustrate the

velocity profile of a (b) Couette flow (b). It is noticed that increasing each of the parameters , Gc, N, Gr, $\mathcal{S}$, Da, λ, and Q increases the velocity profile u, whilst increasing t M, $Sc, Sr, Pe, \mathcal{F}, \varepsilon, Re$, and ω. Because the upper wall of the channel moves at a constant velocity (U 0=0.3), the fluid flow velocity in Couette flow is greater than that of Poiseuille flow. This is why the highest value of the fluid velocity in Poiseuille flow is in the middle of the flow channel, while the highest value of the speed in Couette flow is at the upper wall.

2. Figures (18-21) illustrate the temperature profile. Figure 18 indicates that as Q increases, the temperature rises. As seen in Figure 19, the temperature drops as rises. The temperature rises as N increases, as seen in Figure 20. In Figure 21, we can observe that as Pe grows, the temperature lowers.
3. Figures 22 depict the focused profile 28. The concentration profile decreases with increasing Q, as seen in figure 22. Figure 23 illustrates that when the value of drops, so does the concentration profile. The concentration profile rises with increasing Pe, as seen in Figure 24. It can be seen in Figure 25 that as N increases, the concentration profile diminishes. It can be seen in Figure 26 that when Sr increases, the concentration profile diminishes. The impact of Sc on the concentration profile may be seen in figure 27 by the increasing Sc, then decreasing Sc. The concentration profile diminishes as Kr increases, as seen in Figure 28.

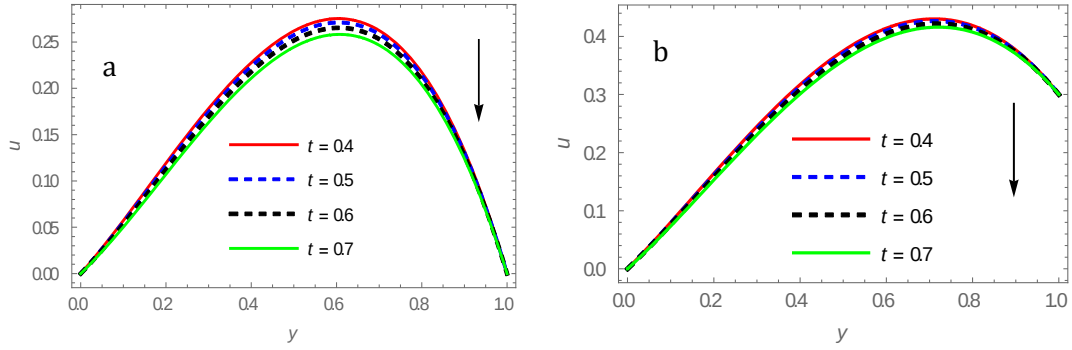

Figure 2 Velocity profile with different values $t = \{0.4,0.5,0.6,0.7\}$ for (a) Poiseuille flow and (b) Couette flow, with $\omega = 1, \lambda = 0.9, \mathrm{Re} = 1, F = 0.5, M = 1, \mathrm{Da} = 1, Sc = 0.6, \mathcal{S} = 0.05, N = 1.25, Q = 2, \delta = \frac{\pi}{4}, Gr = 1, Sr = 0.1, Sr = 0.1, Pe = 2, U_0 = 0.3$.

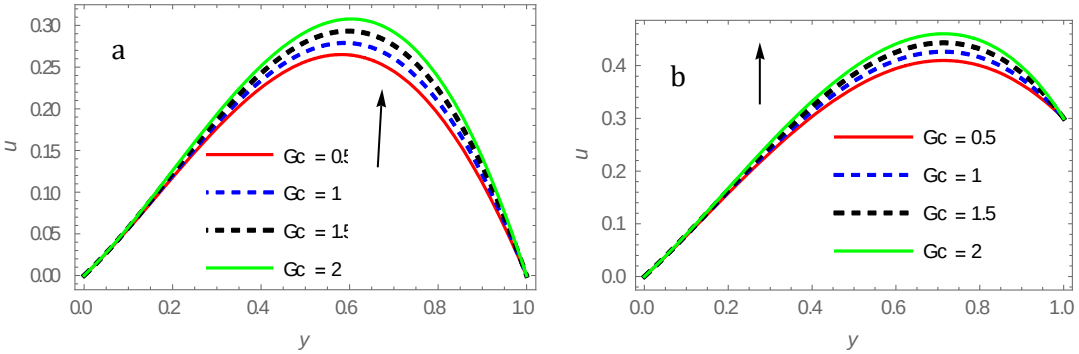

Figure 3 Velocity profile with different values $\mathrm{Gc} = \{0.5,1,1.5,2\}$ for (a) Poiseuille flow and (b) Couette flow, with $\omega = 1, \lambda = 0.9, \mathrm{Re} = 1, F = 0.5, M = 1, \mathrm{Da} = 1, \mathcal{S} = 0.05, N = 1.25, \mathrm{Gc} = 1, Gr = 1, Q = 2, \delta = \frac{\pi}{4}, Pe = 2, Sc = 0.6, Sr = 0.1, t = 0.5, U_0 = 0.3$.

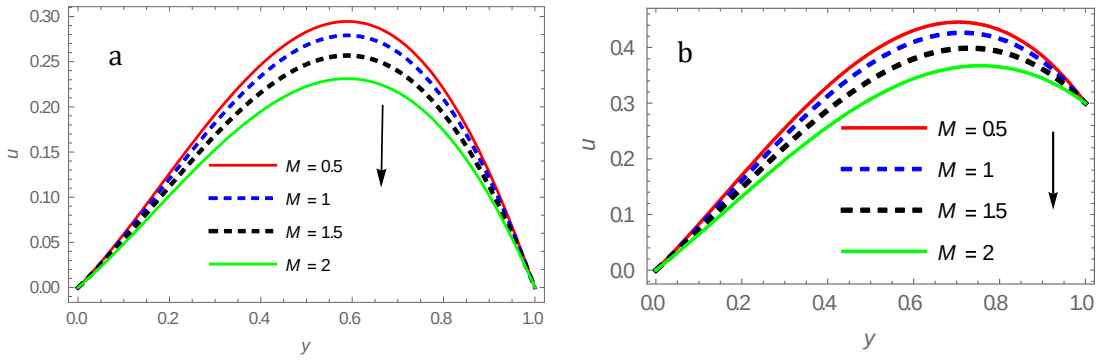

Figure 4 Velocity profile with different values $M = \{0.8,1,1.2,1.4\}$ for (a) Poiseuille flow and (b) Couette flow, with $\omega = 1, t = 0.5, F = 0.5, \lambda = 0.9, \mathrm{Re} = 1, \mathrm{Da} = 1, \mathcal{S} = 0.05, Gr = 1, Q = 2, \delta = \frac{\pi}{4}, Pe = 2, N = 1.25, Sc = 0.6, \mathrm{Gc} = 1, Sr = 0.1, U_0 = 0.3$

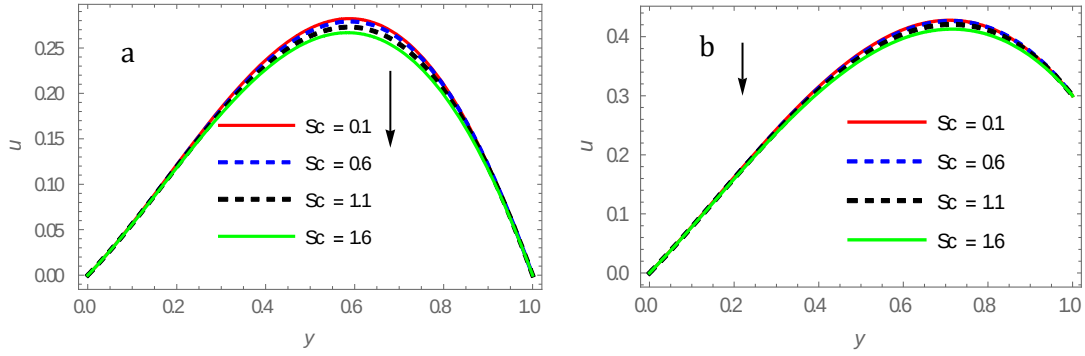

Figure 5 Velocity profile with different values$Sc = \{0.1,0.6,1.1,1.6\}$ for (a) Poiseuille flow and (b) Couette flow, with $\omega = 1, t = 0.5, F = 0.5, \lambda = 0.9, \mathrm{Re} = 1, \mathrm{Da} = 1, \mathcal{S} = 0.05, Gr = 1, Pe = 2, M = 1, Q = 2, \delta = \frac{\pi}{4}, Sr = 0.1, N = 1.25, \mathrm{Gc} = 1, U_0 = 0.3.$

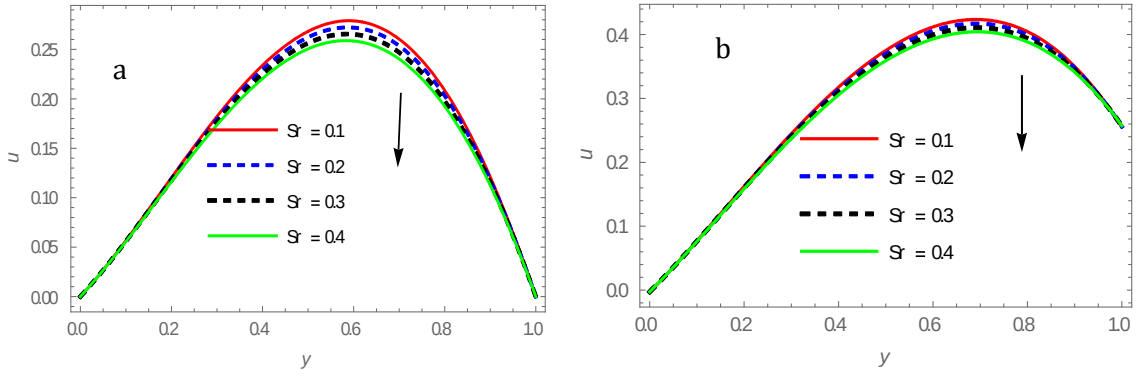

Figure 6 Velocity profile with different values$Sr = \{0.1,0.2,0.3,0.4\}$ for (a) Poiseuille flow and (b) Couette flow, with $\omega = 1, t = 0.5, F = 0.5, \lambda = 0.9, \mathrm{Re} = 1, \mathrm{Da} = 1, \mathcal{S} = 0.05, Gr = 1, Pe = 2, N = 1.25, Sc = 0.6, M = 1, Q = 2, \delta = \frac{\pi}{4}, \mathrm{Gc} = 1, U_0 = 0.3.$

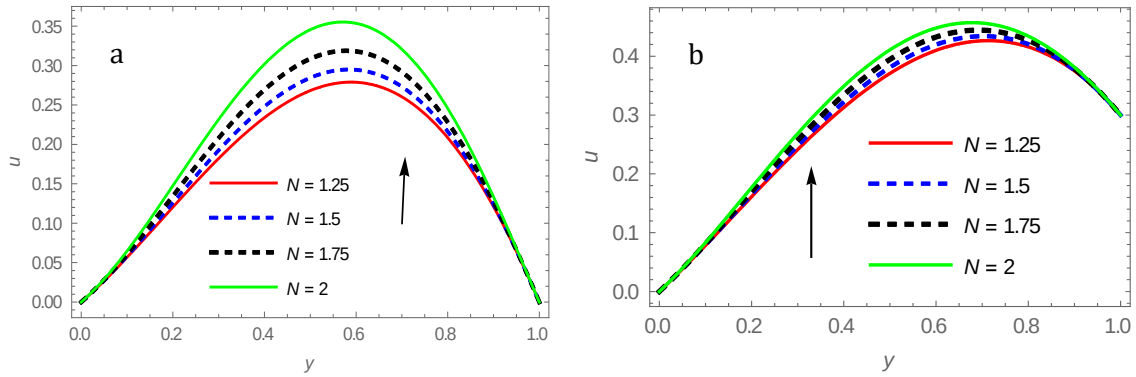

Figure 7 Velocity profile with different values$N = \{1.25,1.5,1.75,2\}$ for (a) Poiseuille flow and (b) Couette flow, with $\omega = 1, Q = 2, \delta = \frac{\pi}{4}, t = 0.5, F = 0.5, \lambda = 0.9, \mathrm{Re} = 1, \mathrm{Da} = 1, \mathcal{S} = 0.05, Gr = 1, Pe = 2, N = 1.25, Sc = 0.6, M = 1, \mathrm{Gc} = 1, U_0 = 0.3.$

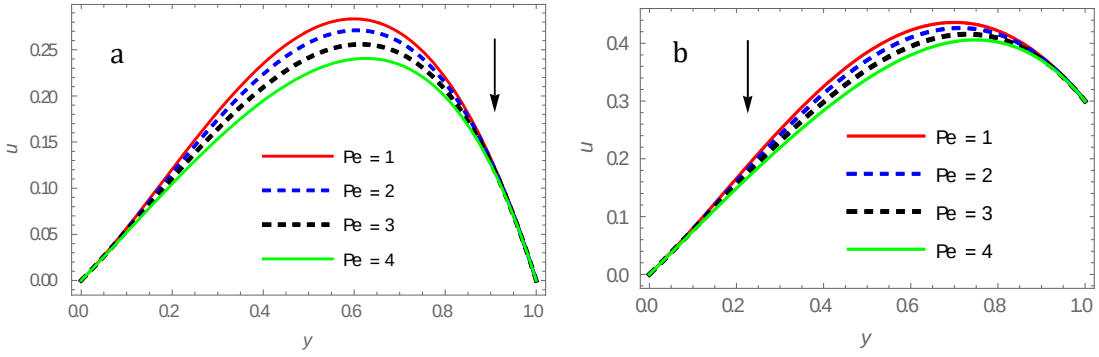

Figure 8 Velocity profile with different values$Pe = \{1,2,3,4\}$for (a) Poiseuille flow and (b) Couette flow, with $\omega = 1, t = 0.5, F = 0.5, \lambda = 0.9, \mathrm{Re} = 1, \mathrm{Da} = 1, \mathcal{S} = 0.05, Gr = 1, Sr = 0.1, Q = 2, \delta = \frac{\pi}{4}, N = 1.25, Sc = 0.6, M = 1, \mathrm{Gc} = 1, U_0 = 0.3.$

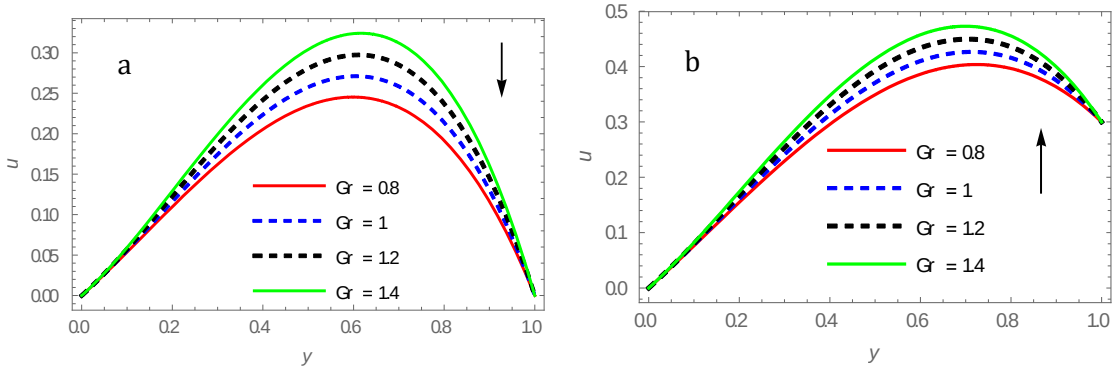

Figure 9 Velocity profile with different values$Gr = \{0.8,1,1.2,1.4\}$for (a) Poiseuille flow and (b) Couette flow, with $\omega = 1, t = 0.5, F = 0.5, \lambda = 0.9, \mathrm{Re} = 1, \mathrm{Da} = 1, \mathcal{S} = 0.05, Pe = 2, Sr = 0.1, N = 1.25, Q = 2, \delta = \frac{\pi}{4}, Sc = 0.6, M = 1, \mathrm{Gc} = 1, U_0 = 0.3.$

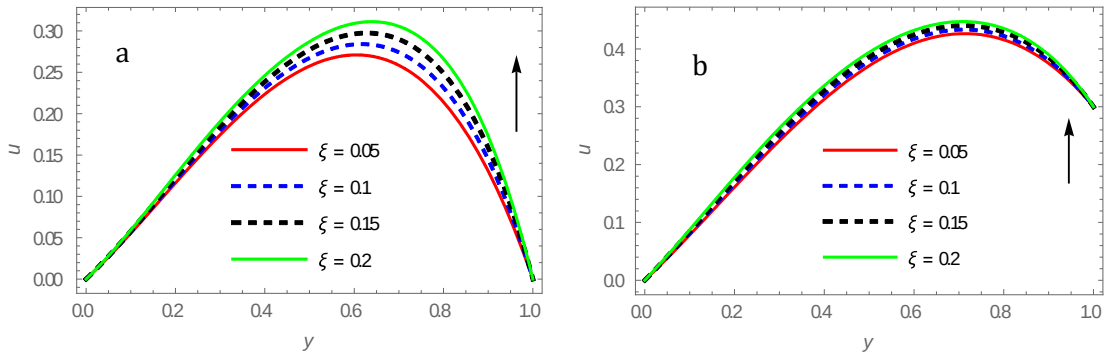

Figuer 10 Velocity profile with different value $\mathcal{S} = \{0.05,0.1,0.15,0.2\}$for (a) Poiseuille flow and (b) Couette flow, with $\omega = 1, t = 0.5, F = 0.5, \lambda = 0.9, \mathrm{Re} = 1, \mathrm{Da} = 1, Gr = 1, Pe = 2, Sr = 0.1, N = 1.25, Q = 2, \delta = \frac{\pi}{4}, Sc = 0.6, M = 1, \mathrm{Gc} = 1, U_0 = 0.3.$

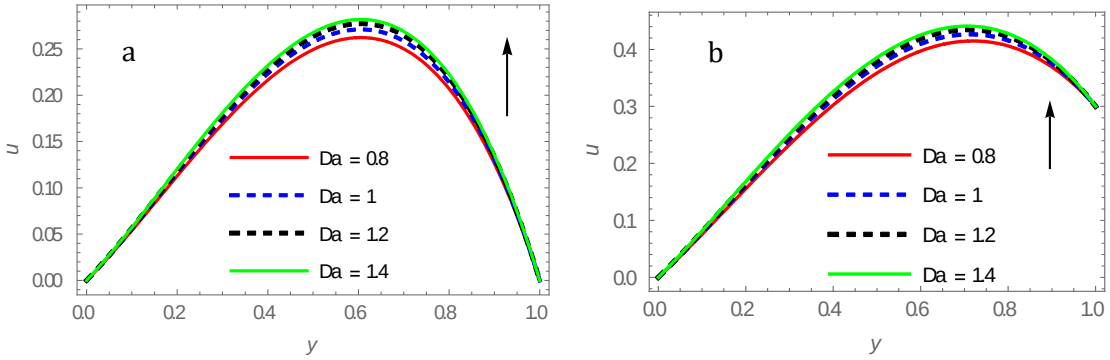

Figure 11 Velocity profile with different value $\mathrm{Da} = \{0.8,1,1.2,1.4\}$for (a) Poiseuille flow and (b) Couette flow, with $\omega = 1, t = 0.5, F = 0.5, \lambda = 0.9, \mathrm{Re} = 1, \mathcal{S} = 0.05, Gr = 1, Pe = 2, Sr = 0.1, N = 1.25, Sc = 0.6, M = 1, \mathrm{Gc} = 1, Q = 2, \delta = \frac{\pi}{4}, U_0 = 0.3.$

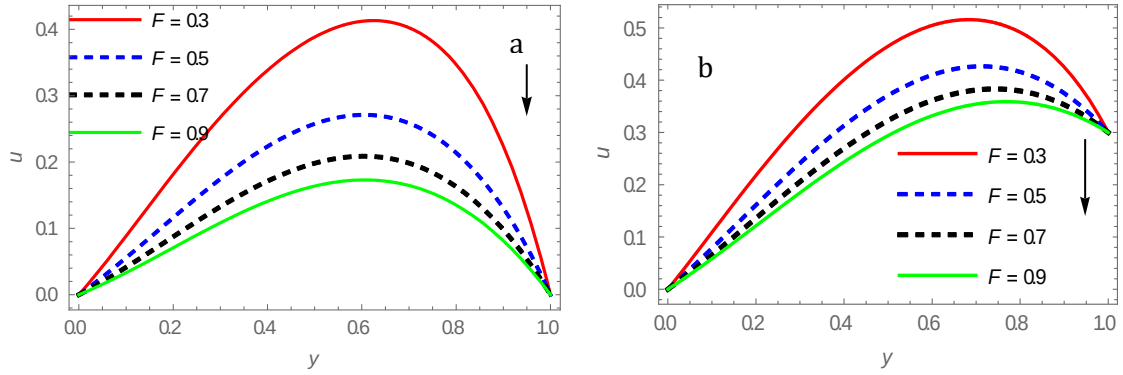

Figure 12 Velocity profile with different value $F = \{0.4,0.5,0.6,0.7\}$ for (a) Poiseuille flow and (b) Couette flow, with $\omega = 1, t = 0.5, \mathrm{Da} = 1, \lambda = 0.9, \mathrm{Re} = 1, \mathcal{S} = 0.05, Gr = 1, Pe = 2, Sr = 0.1, N = 1.25, Sc = 0.6, M = 1, Q = 2, \delta = \frac{\pi}{4}, \mathrm{Gc} = 1, U_0 = 0.3$

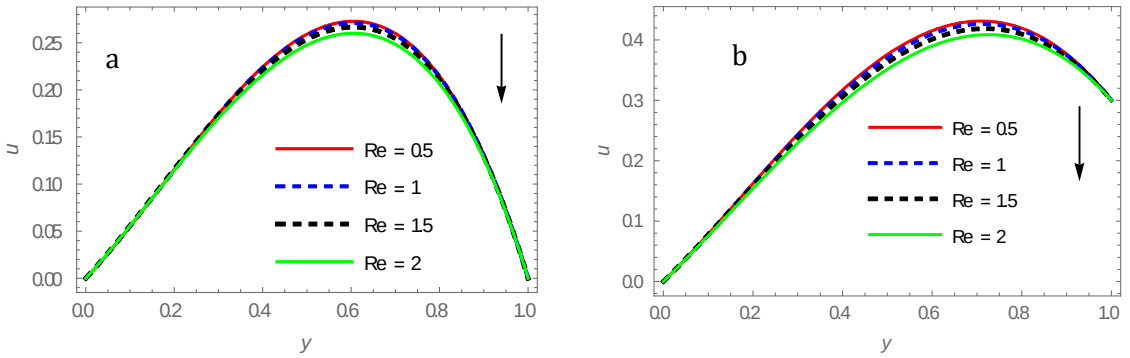

Figure 13 Velocity profile with different value Re = {0.5,1,1.5,2} for (a) Poiseuille flow and (b) Couette flow, with $\omega = 1, t = 0.5, \mathrm{Da} = 1, \lambda = 0.9, \mathcal{S} = 0.05, Gr = 1, Pe = 2, Sr = 0.1, N = 1.25, Q = 2, \delta = \frac{\pi}{4}, Sc = 0.6, M = 1, \mathrm{Gc} = 1, F = 0.5, U_0 = 0.3.$

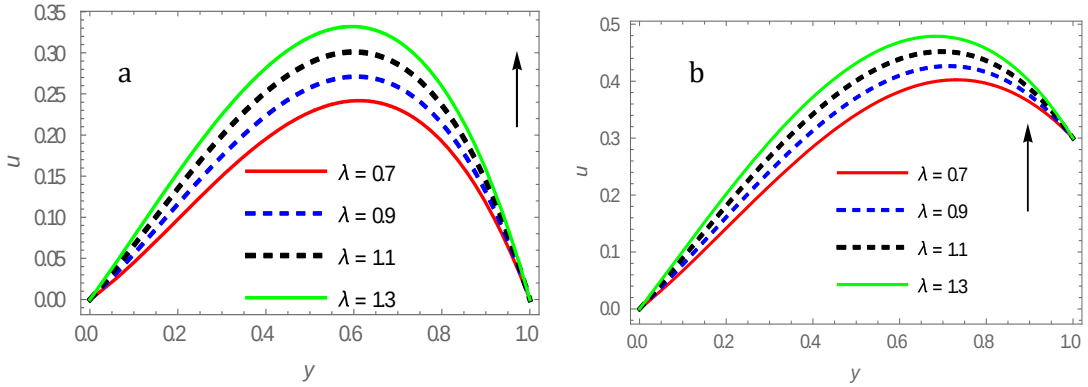

Figure 14 Velocity profile with different value $\lambda = \{0.7, 0.9, 1.1, 1.3\}$ for (a) Poiseuille flow and (b) Couette flow, with $\omega = 1, t = 0.5, \mathrm{Da} = 1, \mathrm{Re} = 1, \mathcal{S} = 0.05, Gr = 1, Pe = 2, Sr = 0.1, Q = 2, N = 1.25, Sc = 0.6, \delta = \frac{\pi}{4}, M = 1, \mathrm{Gc} = 1, F = 0.5, U_0 = 0.3.$

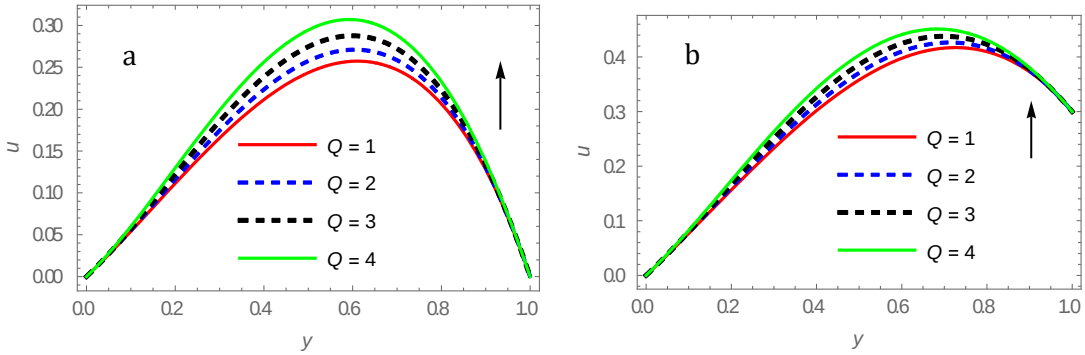

Figure 15 Velocity profile with different value $Q = \{1,2,3,4\}$ for (a) Poiseuille flow and (b) Couette flow, with $\omega = 1, t = 0.5, \mathrm{Da} = 1, \mathrm{Re} = 1, \xi = 0.05, Gr = 1, Pe = 2, Sr = 0.1, N = 1.25, Sc = 0.6, M = 1, \delta = \frac{\pi}{4}, \lambda = 0.9, \mathrm{Gc} = 1, F = 0.5, U_0 = 0.3.$

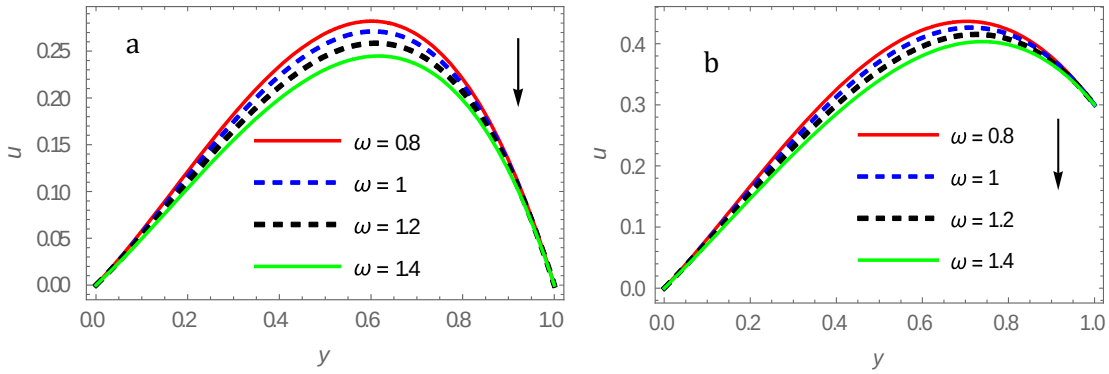

Figure 16 Velocity profile with different value $\omega = \{0.8,1,1.2,1.4\}$ for (a) Poiseuille flow and (b) Couette flow, with $Q = 2, t = 0.5, \mathrm{Da} = 1, \mathrm{Re} = 1, \xi = 0.05, Gr = 1, Pe = 2, Sr = 0.1, N = 1.25, \delta = \frac{\pi}{4}, Sc = 0.6, M = 1, \lambda = 0.9, \mathrm{Gc} = 1, F = 0.5, U_0 = 0.3.$

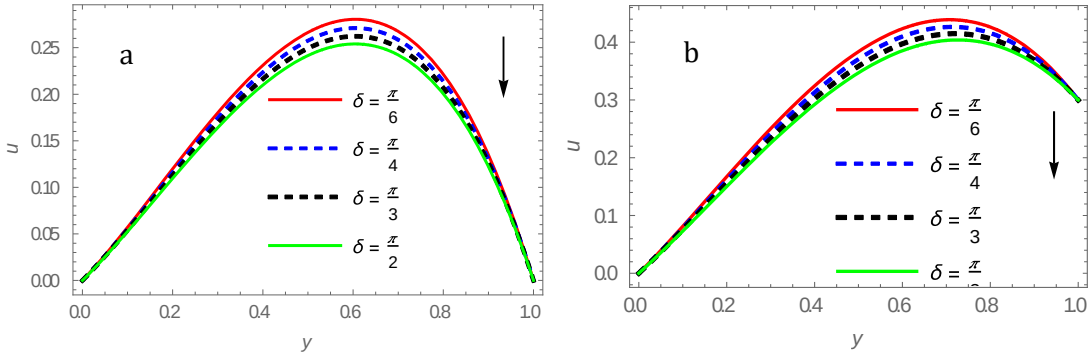

Figure 17 Velocity profile with different value $\delta = \left\{\frac{\pi}{6}, \frac{\pi}{4}, \frac{\pi}{3}, \frac{\pi}{2}\right\}$ for (a) Poiseuille flow and (b) Couette flow, with $Q = 2, t = 0.5, \mathrm{Da} = 1, \mathrm{Re} = 1, \xi = 0.05, Gr = 1, Pe = 2, Sr = 0.1, N = 1.25, Sc = 0.6, M = 1, , \lambda = 0.9, \mathrm{Gc} = 1, F = 0.5, \omega = 1, U_0 = 0.3.$

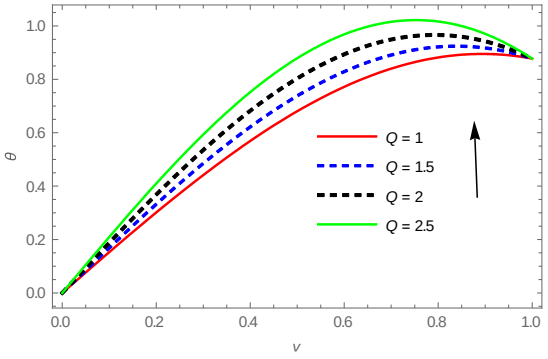

Figure 18 Influence of Q on Temperature for $\omega = 1, N = 1.25, t = 0.0.5, Pe = 2.$

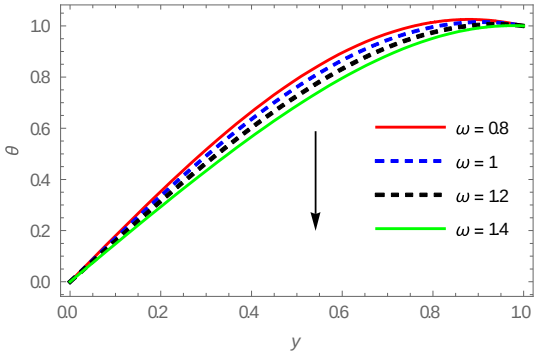

Figure 19 Influence of ω on Temperature for $t = 0.5, N = 1.25, Q = 2, Pe = 2.$

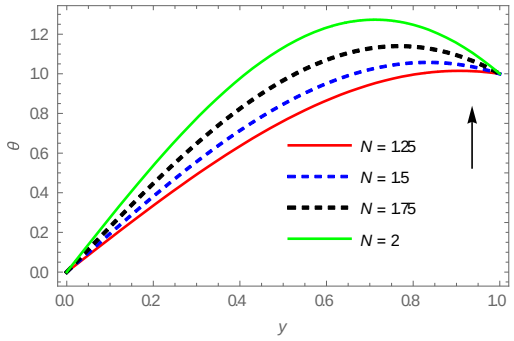

Figure 20 Influence of N on Temperature for $t = 0.5, \omega = 1, Q = 2, Pe = 2.$

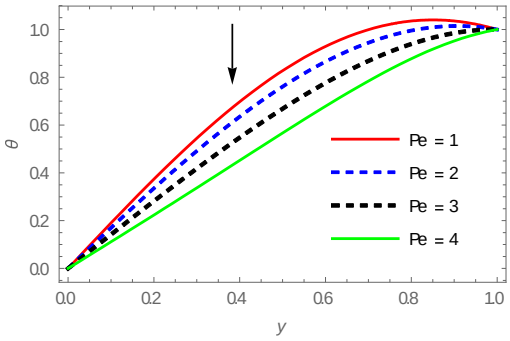

Figure 21 Influence of Pe on Temperature for $t = 0.5, \omega = 1, Q = 2, N = 1.25.$

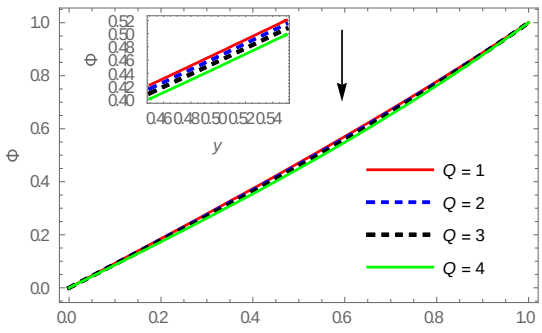

Figure 22 Influence of Q on concentration for $\omega = 1, R = 2,$ Pe = 2, $\mathrm{Sr} = 0.1, \mathrm{Sc} = 0.6, \mathrm{Kr} = 0.5, t = 0.5,$ N = 1.25.

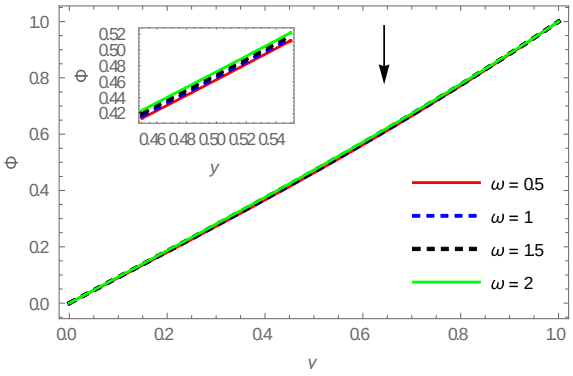

Figure 23 Influence of ω on concentration for $Q = 2, R = 2,$ Pe = 2, $\mathrm{Sr} = 0.1, \mathrm{Sc} = 0.6, \mathrm{Kr} = 0.5, t = 0.5,$ N = 1.25.

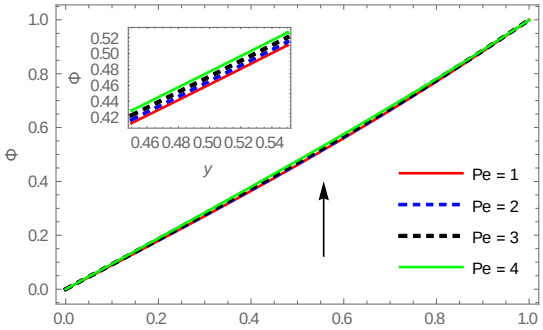

Figure 24 Influence of Pe on concentration for $Q = 2, t = 0.5, R = 2,$ Pe = 2, $\mathrm{Sr} = 0.1, \mathrm{Sc} = 0.6, \mathrm{Kr} = 0.5, \omega = 1,$ N = 1.25.

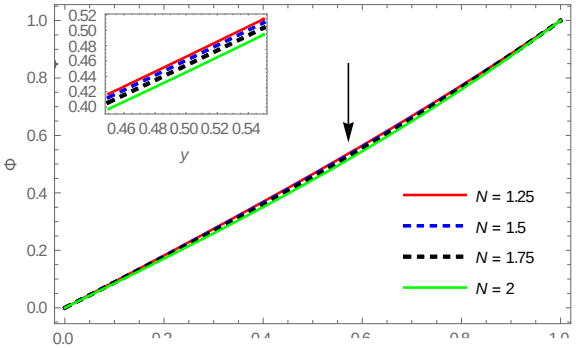

Figure 25 Influence of N on concentration for $Q = 2, t = 0.5, R = 2,$ Pe = 2, $\mathrm{Sr} = 0.1, \mathrm{Sc} = 0.6, \mathrm{Kr} = 0.5, \omega = 1.$

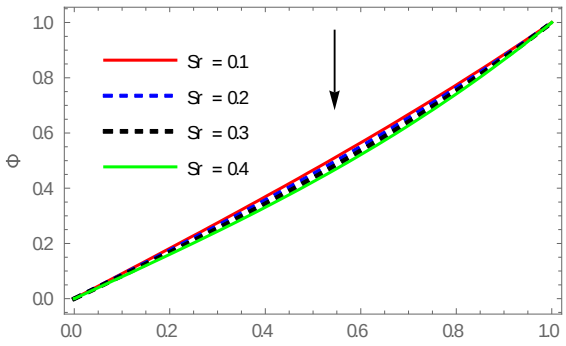

Figure 26 Influence of Sr on concentration for $Q = 2, t = 0.5, R = 2, \mathrm{Pe} = 2, \mathrm{N} = 1.25, \mathrm{Sc} = 0.6, \mathrm{Kr} = 0.5, \omega = 1.$

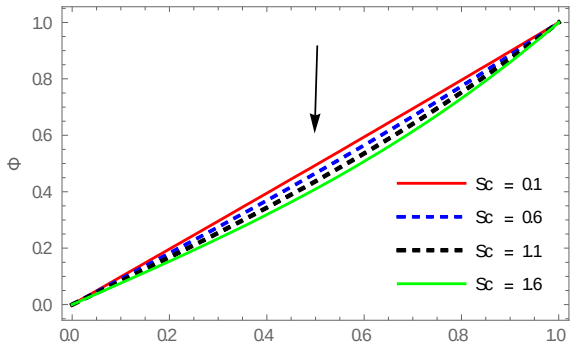

Figure 27 Influence of Sc on concentration for $Q = 2, t = 0.5, R = 2, \mathrm{Pe} = 2, \mathrm{N} = 1.25, \mathrm{Sr} = 0.1, \mathrm{Kr} = 0.5, \omega = 1.$

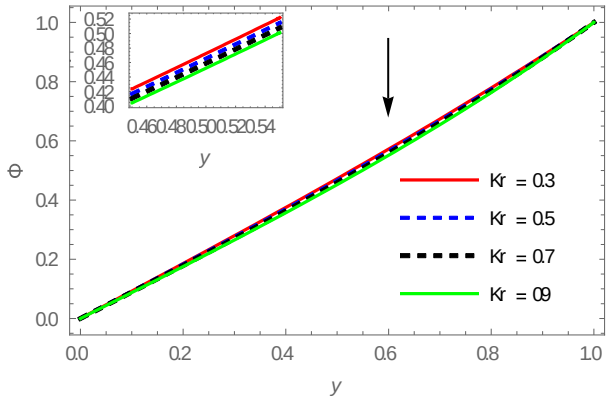

Figure 28 Influence of Kr on concentration for $Q = 2, t = 0.5, R = 2, \mathrm{Pe} = 2, \mathrm{N} = 1.25, \mathrm{Sr} = 0.1, \mathrm{Sc} = 0.6, \mathrm{Kr} = 0.5, \omega = 1.$

7. Conclusion:

The effect of heat transfer on Prandtl-Eyring fluid MHD oscillatory flow through a porous medium with changing temperature and concentration is discussed. We discovered the velocity, temperature, and concentration using the perturbation approach. The findings of relevant parameters, such as the Darcy number and the radiation parameter, are calculated using various values, Magnetic parameter, Soret number, Schmidt number, Peclet number, Grashof number, Schmidt number, Peclet number, Peclet number, Peclet number, Peclet number, Peclet number, Peclet number Some of

the terminology used include Prandtl-Eyring fluid parameters, heat generation parameter, Soret number, oscillation frequency, and Reynold number..

- The velocity of two forms of flow, Poiseuille and Couette, rises when the parameters N, Gr, Gc, λ, Da, Q and s increase, whereas the velocity decreases with the parameters ω, F, ξ, Sr, Sc, $t, Re,$ Pe and M increase.
- Increases in N and Q raise the temperature, whereas increases in and Pe lower it.
- With an increase in Pe, the concentration rises. With the rise of all parameters, ω, N, Q, Sr, Sc, Kr and t, the concentration falls.

Refrains

[1] Arif Hussain, M.Y. Malik, M. Awais, T. Salahuddin, S. Bilal, **2019**, Computational and physical aspects of MHD Prandtl-Eyring fluid flow analysis over a stretching sheet, Neural Comput & Applic 31, 425–433. https://doi.org/10.1007/s00521-017-3017-5.

[2] Dheia G Salih Al –Khafajy, Lqaa Tareq Hadi. **2020**. Influence of Heat Transfer on MHD Oscillatory Flow for Eyring-Powell Fluid through a Porous Medium with Varying Temperature and Concentration. Iraqi J. Sci., Vol. 61, No. 12, pp: 3355-3365

[3] Dheia G. Salih Al-Khafajy, **2020**, Radiation and Mass Transfer Effects on MHD Oscillatory Flow for Carreau Fluid through an Inclined Porous Channel, Iraqi Journal of Science, 61(6),1426-1432. https://doi.org/10.24996/ijs.2020.61.6.21

[4] Hamza, M.M., Isah, B.Y. and Usman, H., **2011**. Unsteady heat-transfer to MHD oscillatory flow during a porous medium under slip condition. International Journal of Computer Applications, 33(4), 12-17.

[5] Hussain H. Z. Farooq M. and Alsaedi M. **2018**; Magnetohydrodynamics flow of Powell-Eyring fluid by a stretching cylinder with newtonian heating, Thermal Science, 22(1B), 371-382.

[6] Javaria Akram, Noreen Sher Akbar, **2020**, Chemical reaction and heat source/sink effect on magnetonano Prandtl-Eyring fluid peristaltic propulsion in an inclined symmetric channel, Chinese Journal of Physics, 65, 300-313. https://doi.org/10.1016/j.cjph.2020.03.004.

[7] Kahshan, M., Lu, D. & Siddiqui, A.M., **2019**, A Jeffrey Fluid Model for a Porous-walled Channel: Application to Flat Plate Dialyzer. Sci Rep 9, 15879.

[8] Khalil Ur Rehman, Aneeqa Ashfaq Malik, M.Y.Malik, M.Tahir, Iffat Zehra, 2018, On new scaling group of transformation for Prandtl-Eyring fluid model with both heat and mass transfer, Results in Physics, 8, 552-558.

[9] Lqaa Tareq Hadi and Dheia G. Salih Al–Khafajy, **2020**. Influence of Heat Transfer MHD Oscillatory Flow for an Eyring-Powell Fluid with Variable Viscosity through a Porous Medium, J. Phys.: Conf. Ser. 1664 012031.

[10] Nabil T. Eldabe, Galal M. Moatimid, Abdelhafeez A. ElShekhipy, Naglaa F. Aballah, **2019**, Mixed convective peristaltic flow of Eyring-Prandtl fluid with chemical reaction and variable electrical conductivity in a tapered asymmetric channel, HEAT TRANSFER, 48(5), 1946-1962,

https://doi.org/10.1002/htj.21466.

[11] Nigamf B. and Singhj S. **1960** ; Heat transfer by laminar flow between parallel plates under the action of transverse magnetic field, Quart. Jour. Mech. Applied. Math, XIII(5).

[12] Panigrahi Lipika, Panda Jayaprakash, Swain Kharabela, Dash Gouranga Charan, **2020**, Heat and mass transfer of MHD Casson nanofluid flow through a porous medium past a stretching sheet with Newtonian heating and chemical reaction, Karbala International Journal of Modern Science, 6(3), Article 11. https://doi.org/10.33640/2405-609X.1740 .

[13] Raptis A., Massias C. and Tzivanidis G., **1982**; Hydromagnetic free convection flow during a porous medium between two parallel plates MHD, Phys. Lett., 90A, 288-289.

[14] Rashid M., Iqra Shahzadi, S. Nadeem, **2018**. Corrugated walls analysis in microchannels through porous medium under Electromagneto-hydrodynamic (EMHD) effects, , Results in Physics, 9, 171-182.

[15] Sharp K.M., Carare R.O. and Martin B.A., **2019**, Dispersion in porous media in oscillatory flow between flat plates: applications to intrathecal, periarterial and paraarterial solute transport in the central nervous system. Fluids Barriers CNS 16, 13.

[16] Siddiquia A.M., Q.A. Azim, **2020**, Creeping flow of a viscous fluid in a uniformly porous slit with porous medium: An application to the diseased renal tubules, Chinese Journal of Physics, 64, 264-277.

[17] Sumaira Qayyum, Tasawar Hayat, Mehreen Kanwal, Ahmed Alsaedi, M.Ijaz Khan, **2020**, Transportation of entropy optimization in radiated chemically dissipative flow of Prandtl–Eyring nanofluid with activation energy, Computer Methods and Programs in Biomedicine, 184, 105130. https://doi.org/10.1016/j.cmpb.2019.105130